Intermittent movement control emerges from information-based planning

Atsushi Takagi[1*†], Dorian Verdel[2*] and Etienne Burdet[2]

[1]Human Information Science Laboratory, NTT Communication Science Laboratories,
Atsugi, Japan
[2]Bioengineering department, Imperial College of Science, Technology and Medicine,
London W12 0BZ, United-Kingdom
*These authors contributed equally
†E-mail: atsushi.takagi@ntt.com

Abstract

Dominant models of reactive motion control in humans, based on optimal feedback control, predict smooth trajectories that reflect averaged behaviors. However, the observation of individual movements suggests that mammalian motor control is inherently discrete, with movement corrections occurring at a rate that depends on task demands and sensory information quality. To address these limitations, we introduce the Information Predictive Control (IPC) framework that integrates model predictive control with information theory, which triggers movement corrections only when unexpected deviations occur and corrections are likely to succeed. By quantifying "surprise" relative to anticipated internal and external states, IPC produces successful movements while robustly responding to sensorimotor noise, task constraints, and target variability. Simulations demonstrate IPC's ability to reproduce human-like responses to novel force fields during reaching, continuous target tracking, and adaptive planning under noise, while dynamically adjusting the planning horizon in complex, unpredictable environments.

1 Introduction

Mammals face the fundamental challenge of planning movement in a dynamic and unpredictable environment. For instance, they must continuously replan their actions to intercept an agile prey or interact efficiently with a dynamic environment. Early attempts to understand the underlying motor planning mechanisms relied on deterministic feed-forward control, optimizing energy or motion smoothness to predict the average trajectory across repeated trials [1–7]. More recent approaches have accounted for inherent sensorimotor noise [8] and random external perturbations [9] to predict movement trajectories in presence of uncertainty. While these open-loop control models perform well when internal and external dynamics change gradually, allowing the brain to build reliable internal models [10], they are not designed to handle sudden changes, such as for catching a fly, or recovering from a stumble after hitting the sidewalk.

In such dynamic situations, the ability to react to task or environmental changes by replanning movement is essential [11, 12]. The continuous correction of deviations from a goal and the associated effort has been modeled using Optimal Feedback Control (OFC) [13, 14]. However, OFC yields a servo mechanism responding to any target movement without distinguishing whether the target is unreachable, due for example to sensory noise or rapid oscillations. Moreover, originally developed for aeronautics, OFC fails to predict key features of mammalian motor control, particularly the submovements observed in cats [15], mice [16], humans [17–19] and non-human primates [20]. These submovements suggest that mammals' sensorimotor control may rely on an intermittent strategy rather than continuous feedback regulation.

Several mechanisms have been proposed to explain movement intermittency in humans. It has been attributed to biological constraints imposing a fixed control frequency [17, 21] or may arise from error sensitivity exceeding a perceptual threshold [22–24]. However, these explanations do not account for observed variations in control frequency due to sensory feedback quality. For instance, movement intermittency decreases when tracking a target with noisy peripheral vision compared to sharp foveal vision [25]. Furthermore, existing models overlook how motor noise and

other sources of deviation influence the rate of replanning. A more comprehensive framework is needed to integrate these factors and explain how movements are dynamically replanned in response to environment changes.

To address these issues, we developed the Information-based Predictive Control (IPC) framework, which incorporates sensory noise, motor noise, task-related constraints, and environmental unpredictability into motor planning. IPC models internal and external states to predict upcoming conditions, guiding optimal actions through a model predictive control scheme [26, 27] with an adaptive planning horizon. We propose that the central nervous system (CNS) monitors deviations between predicted and actual states, triggering movement replanning when discrepancies exceed a perceptual threshold—quantified using Shannon entropy [28] (Fig. 1). Through simulations and comparisons with experimental data, we demonstrate how IPC generates human-like responses in diverse motor tasks, including reaching in a force field, continuous target tracking, adaptive planning under motor noise constraints, and a hunting task involving prey with varying agility.

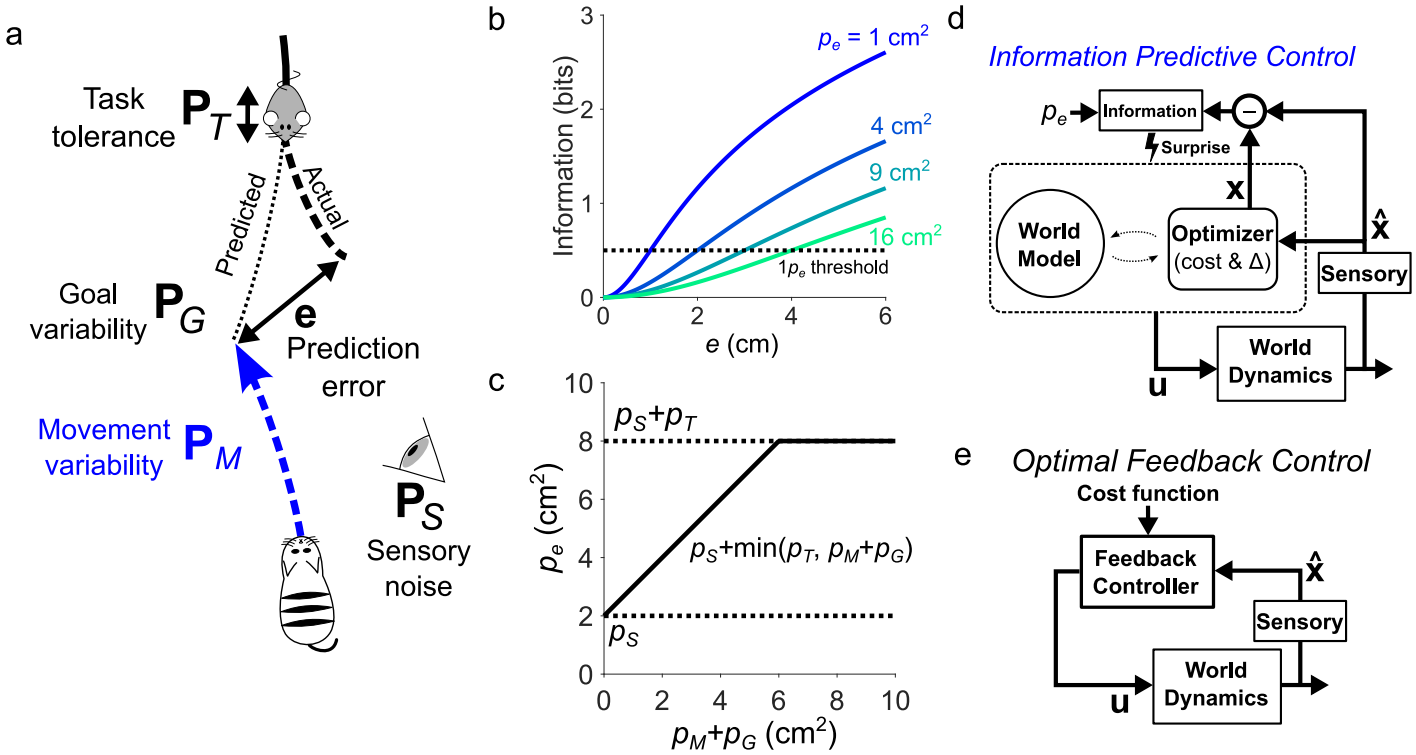

Figure 1: Planning and correction of movements under IPC and OFC. (a) Schematic of a hunter intercepting a prey. The hunter must predict the prey's movement to intercept the prey, but if either the prey or the hunter's movement deviates from the planned trajectory, then a new movement must be replanned. Replanning should consider sensory noise $\mathbf{P}_S$, the variability of IPC's movement $\mathbf{P}_M$ and the goal's movement $\mathbf{P}_G$, and the task tolerance $\mathbf{P}_T$. (b) Information as a function of prediction error for different permissible variance values. As the permissible variance $\mathbf{P}_e$ increases (here with only one-dimensional position deviations for the sake of simplicity, i.e. $p_e = \mathbf{P}_e \in \mathbb{R}$), IPC deems the same prediction error to be less surprising. (c) Permissible variance in the prediction error p_e is capped by the task tolerance p_T. Below this point, p_e is a function of $p_M + p_G$. Sensory noise p_S offsets the entire function. (d) Schematic of IPC. When the predicted and measured states deviate and generate enough information to create a surprise, IPC replans a new movement using optimization and a forward model of the dynamics. (e) OFC uses an optimal feedback gain that provides continuously corrects for deviations from the planned trajectory.

2 Results

IPC provides a general principle for reactive control, yielding intermittent motor replanning with an adaptive time horizon when it is necessary and feasible, considering the level of sensory noise, task constraints, movement variability due to motor noise and the target movement variability (Fig. 1a). IPC generates movement to minimize the distance between its own state $\mathbf{x}$ and the goal state $\mathbf{x}^*$ with minimal effort, where the state of dimension N may include position, velocity, force, etc. Critically, IPC intervenes in an ongoing movement only when a significant change occurs, as analyzed from the prediction error [29, 30]

$$\mathbf{e} = (\mathbf{x} - \mathbf{x}^*) - (\hat{\mathbf{x}} - \hat{\mathbf{x}}^*) \tag{1}$$

between the current and measured states $\hat{\mathbf{x}}$ and $\hat{\mathbf{x}}^*$. Specifically, when the Shannon information [28]

$$I = 0.5 \log_2 \left(1 + \sum_{i=1}^{N} \frac{e_i^2}{\mathbf{p}_{e,i}} \right) \tag{2}$$

exceeds a threshold I_T, where $\mathbf{p}_e$ is the permissible state variance vector, IPC considers the movement to have significantly deviated from its prediction and triggers motion replanning. In this study we set I_T=0.5, meaning that a deviation exceeding one standard deviation of the prediction error is considered sufficiently "surprising" to initiate replanning.

As illustrated in Fig. 1b, when $\mathbf{p}_e$ components are small, even minor prediction errors generate high information values, making IPC more sensitive to deviations. The amount of information generated by the *prediction error* $\mathbf{e}$, computed from

$$\mathbf{p}_e = \mathrm{diag}\left(\mathbf{P}_e\right) \ , \quad \mathbf{P}_e = \mathbf{P}_S + \min\left(\mathbf{P}_T, \mathbf{P}_M + \mathbf{P}_G\right) \tag{3}$$

depends on sensory noise (where $\mathbf{p}_S = \mathrm{diag}\left(\mathbf{P}_S\right)$ are the corresponding variance vector and covariance matrix), task tolerance (with $\mathbf{p}_T = \mathrm{diag}\left(\mathbf{P}_T\right)$), on IPC's movement variability (via $\mathbf{p}_M = \mathrm{diag}\left(\mathbf{P}_M\right)$), and on the goal's variability (with $\mathbf{p}_G = \mathrm{diag}\left(\mathbf{P}_G\right)$), where the respective sources of variability are assumed to be independent stochastic variables. Fig. 1c illustrates how these four factors influence the permissible variance. An increase in sensory noise reduces the reliability of the prediction error estimate, making IPC less likely to trigger replanning. Similarly, as movement variability and goal variability increase, replanning becomes less likely—until they exceed the task constraint variability. This allows movement and goal variability to grow with no replanning until it interferes with the task, i.e. minimum intervention [13, 31]. Beyond this threshold, further increases in movement or goal variability raise the likelihood of replanning, as the prediction error surpasses the permissible variance more often. If IPC's predictions are accurate, the predicted error will be sufficiently small so as to not require replanning (Fig. 1a). However, when sensorimotor noise or unexpected target motion occurs, prediction errors grow over time, necessitating replanning.

2.1 Movement planning by IPC

We assume that the brain maintains an internal model of the task dynamics $\dot{\mathbf{x}} = \mathbf{f}\left(\mathbf{x},\ \mathbf{u}\right)$ and $\dot{\mathbf{x}}^* = \mathbf{f}\left(\mathbf{x}^*, \mathbf{u}^*\right)$ where $\mathbf{u}$ is the control vector of the system containing, e.g., joint torques or muscle activations. This internal model enables the brain to predict the trajectory of the goal state $\mathbf{x}^*$ and plan optimal actions over a *finite time horizon* $\triangle$, depending on the defined system variances. The learning of this internal model by the brain—incorporating system dynamics and the four sources of variability—is beyond the scope of this study and could be explained by Bayesian inference [32] or active inference [33] frameworks. Given this internal model, the brain plans optimal actions by minimizing a cost function over $\triangle$

$$V(t) = \int_t^{t+\triangle} l(\mathbf{x}, \mathbf{u}, \zeta)\, d\zeta \tag{4}$$

where t is the current time of replanning, and $l(\mathbf{x}, \mathbf{u}, \zeta)$ represents a cost function modeling human behavior, e.g. a quadratic function of error to the target and the effort required to reach it (see Methods for details on cost functions used in simulations).

2.2 Movement replanning while reaching under perturbations

2.2.1 Replanning during arm reaching in a novel force field

We now examine IPC's performance in increasingly complex scenarios, starting with a simple arm-reaching task. For simplicity, in the remainder of this manuscript, only stochasticity in position is considered, reducing the state vector and $\mathbf{P}_e$ matrix to position alone. Fig. 2b illustrates a reaching movement in a horizontal plane towards a target (represented as a disk), simulated using IPC and OFC (see Methods for details). The dotted line in the top panel of Fig. 2c shows unperturbed movements, which follow a straight-line trajectory in the task space with a bell-shaped speed profile under both IPC and OFC.

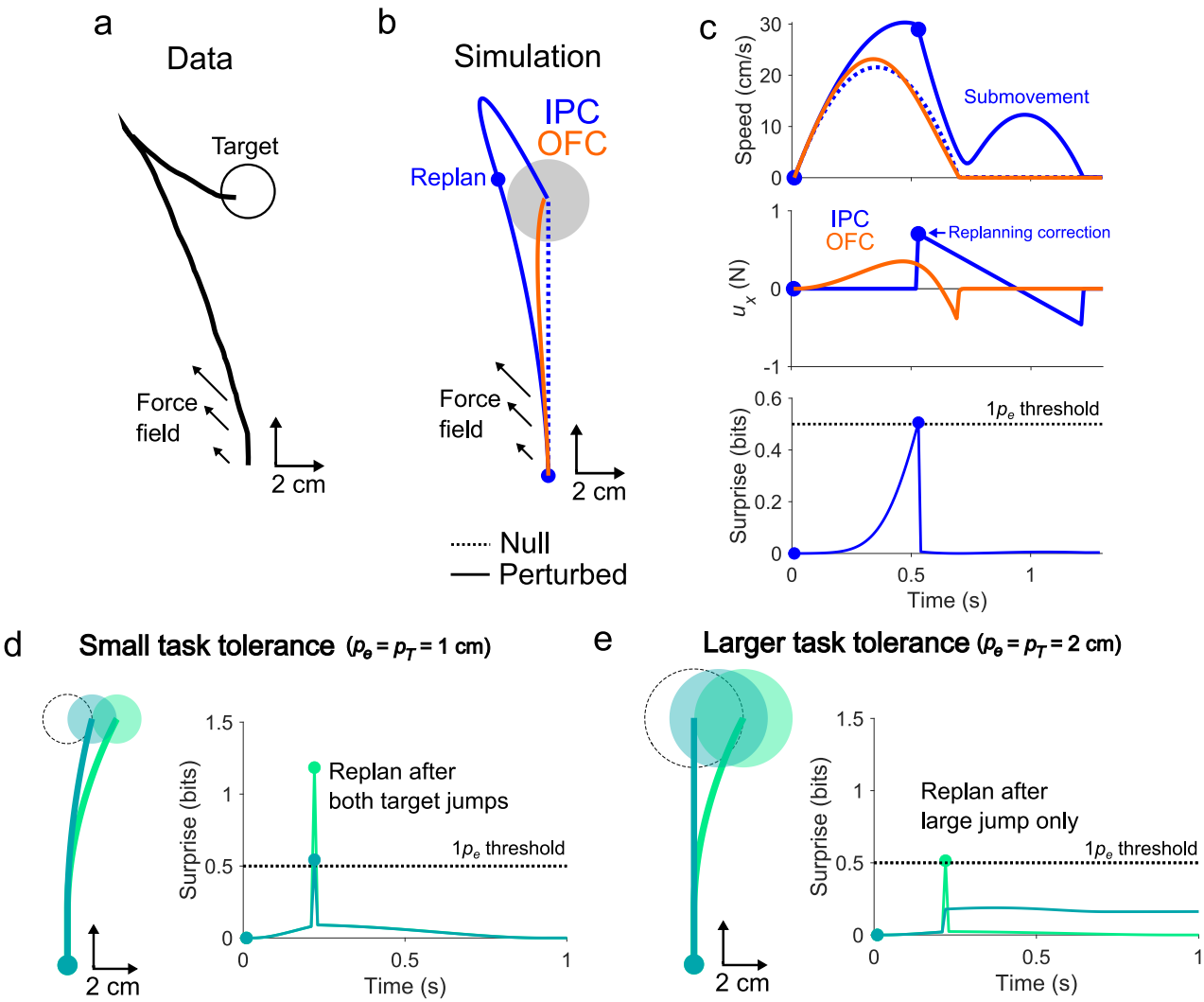

Figure 2: IPC only replans a new movement after large surprise, while OFC continuously corrects prediction errors of any size. (a) Trajectory of a participant reaching a target when perturbed by a novel velocity-dependent force field (adapted from [34]). The force field (arrows) pushes laterally and forwards, causing an overshoot, before eventually returning to the target. (b) Reaching without (dashed) and with a perturbation from a velocity-dependent force field (solid lines). OFC reaches practically straight like in the null field, while IPC overshoots and corrects its movement to reach the target like in the data ($p_e = 9\,\mathrm{cm}^2$). (c) In response to the force field, OFC reacts quickly and pushes laterally against the force field to return to the nominal trajectory (middle panel). IPC replans an executes a new movement once the measured position deviates significantly from the predicted trajectory, generating large surprise (bottom panel). The newly planned correctional movement is visible as a submovement with its own velocity peak (top panel). (d) IPC's reaction to target jumps when the task tolerance is $p_e = p_T = 1\,\mathrm{cm}^2$. Even the smallest $1\,\mathrm{cm}$ target jump elicits a sufficiently large surprise to trigger replanning to the new target location. (e) When IPC's task tolerance is $p_e = 4\,\mathrm{cm}^2$, it only replans its movement after the larger $2\,\mathrm{cm}$ target jump and not after the smaller $1\,\mathrm{cm}$ target jump.

How do IPC and OFC respond to a novel force field applied on the hand during movement [34]? Fig. 2a depicts the reaction of a representative participant to this velocity-dependent force field in the experiment of [34]. The hand initially overshoots the target and deviates to the left, before correcting its trajectory towards the target. In simulations, OFC (orange trace) continuously counteracts the force field as soon as the deviation occurs (middle panel of Fig. 2c). As a result, OFC maintains a trajectory close to the original plan (dotted trace in Fig. 2c). In contrast, IPC initially deviates significantly from the originally planned trajectory (dashed line). However, as prediction error accumulates, the associated Shannon information rapidly increases (solid blue traces in Fig. 2b,c). Once this information surpasses the surprise threshold (bottom panel of Fig. 2c), IPC triggers a movement replanning with a corrective force to redirect the hand toward the target. Consequently, the lateral force to counteract the external force field emerges with a delay, depending on the information from task-related deviations (middle panel of Fig. 2c, blue trace). This corrective movement manifests as a second peak in the speed time series, commonly referred to as a submovement. While IPC exhibits such

discrete submovements in response to an unexpected force perturbation, OFC corrects the deviation continuously and smoothly.

The different responses with OFC and IPC arise from their underlying control policies (Fig. 1d,e). In OFC, the servo control policy relies on an optimal feedback gain multiplied by the state error, the difference between the current and target position. Even when accounting for sensory delays, OFC would still generate a continuous, albeit delayed, corrective movement without discrete submovements. In contrast, IPC follows an iterative open-loop control strategy to perform movement. Because IPC relies on local, intermittent replanning without immediate feedback-based corrections, it cannot react instantaneously to unexpected perturbations. Instead, it generates discrete corrections, only when deemed necessary. Note that, if the perturbation was known beforehand, then IPC would simply compensate it in open-loop, resulting in straight arm reaching trajectories as observed in stable conditions, e.g. after learning [35].

2.2.2 Effect of task tolerance on IPC's reaction to target jumps

To investigate the influence of the task permissible variance, we varied p_T while analyzing IPC's response to abrupt lateral target displacements (Fig. 2d). We simulated IPC's reaction to two target jumps with different magnitudes. With the task tolerance $p_T = 1\,\mathrm{cm}^2$ both target jumps generated sufficient surprise to trigger movement replanning toward the new target location. With the larger task tolerance $p_T = 4\,\mathrm{cm}^2$ only the $2\,\mathrm{cm}$ target jump was surprising, whereas the $1\,\mathrm{cm}$ jump did not elicit a corrective response (Fig. 2e). This result shows how IPC's replanning frequency – and consequently, the intermittency of movements – depends on task tolerance: smaller tolerances lead to more frequent and discrete corrective adjustments.

2.3 Human-like submovements in continuous tracking

IPC also replicates the intermittent corrections observed in humans continuously tracking targets [36]. In this task, human participants tracked a randomly moving target by flexing and extending the wrist (Fig. 3a; see Methods for details).

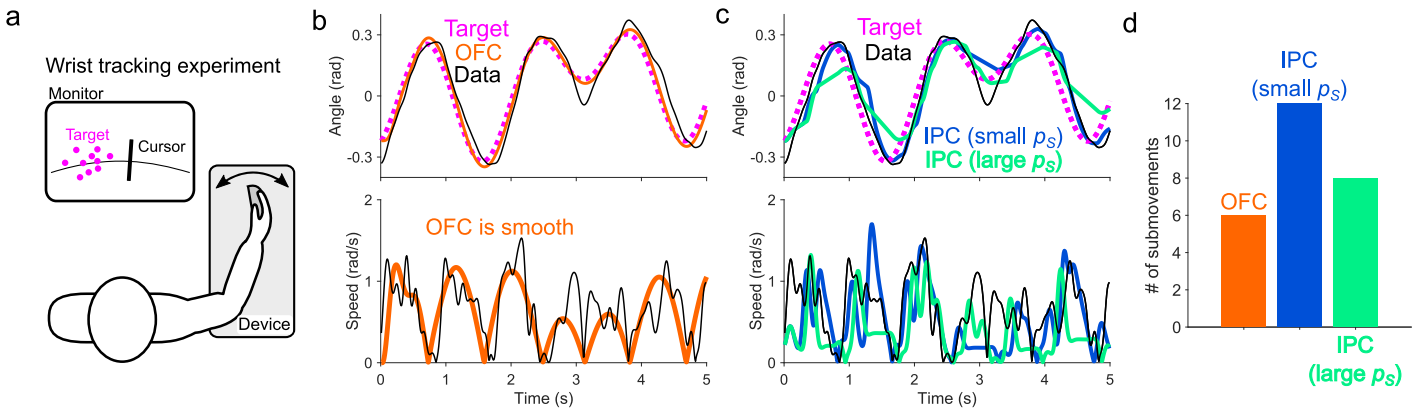

Figure 3: IPC generates submovements when tracking a randomly moving target. (a) Participants tracked a smoothly moving target using their wrist as accurately as possible. (b) Angle (top) and speed time-series (bottom panel) when tracking a target (magenta). Data (black dotted trace) is from one participant from a five second slice of a forty second trial. When tracking the target, OFC tracks the target with a smooth speed profile (orange). However, the participant used submovements when tracking, which is visible as multiple bumps in the speed time-series (black). (c) IPC tracking the same target trajectory with a task tolerance $p_T = 8\,\mathrm{cm}^2$ and low sensory noise $p_S = 8\,\mathrm{cm}^2$ (blue) or high sensory noise $p_S = 56\,\mathrm{cm}^2$ (green). IPC is more accurate at tracking the target and exhibits a larger number of peaks in speed when sensory noise is small. With large sensory noise, IPC produces fewer seed peaks and is less accurate at tracking. (d) Number of submovements in the tracking simulation of (b) and (c) counted by the prominence in the speed peaks. IPC with the smallest sensory noise had the greatest number of submovements and OFC the fewest, with only submovements imposed by the trajectory.

Fig. 3b shows the speed time series of wrist angle of a representative participant exhibiting multiple submovements characterized by narrow peaks. We simulated this task with both OFC and IPC to test how they would account for these submovements. While OFC generated a smooth continuous tracking trajectory (Fig. 3b,d, orange trace), IPC produced trajectories with multiple submovements as in the experimental data, evidenced by the narrow speed peaks in Fig. 3c.

We further explored IPC's predictions by varying sensory noise and analyzing its effect on tracking accuracy and the frequency of submovements. As shown in Fig. 3d, large sensory noise ($p_S = 56\,\mathrm{cm}^2$) leads to a low tracking accuracy and few submovements, as less information is available, while small sensory noise ($p_S = 8\,\mathrm{cm}^2$) leads to high accuracy and frequent submovements, as unwanted deviations are better detected. Thus, IPC's replanning mechanism based on information accounts for the observed intermittent corrections during continuous tracking and predicts changes in motor behavior as a function of sensory information [25].

2.4 Evolution of the optimal planning horizon in the face of uncertainty

IPC plans and replans a movement for a future duration set by the time horizon $\triangle$. How large should this horizon be, and what factors influence it? Here, we consider two factors: the cost of transport in Eq. 4 and prediction uncertainty (Fig. 4a). The effect of the cost of transport on the optimal horizon is illustrated by a simulation of a reaching movement to a static target (Fig. 4b, left). In that case, the horizon can be chosen equal to the movement duration as the CNS can easily plan such simple reaching tasks at once. Consequently, shorter movement duration will be associated with higher cost of transport. Therefore, in absence of any complementary costs (e.g. related to time or additive motor noise [37]), the optimal horizon (i.e. movement duration) would tend to infinity (Fig. 4b, right). In practice, such complementary costs could explain why a very long horizon is not used by the CNS, as described in the Discussion.

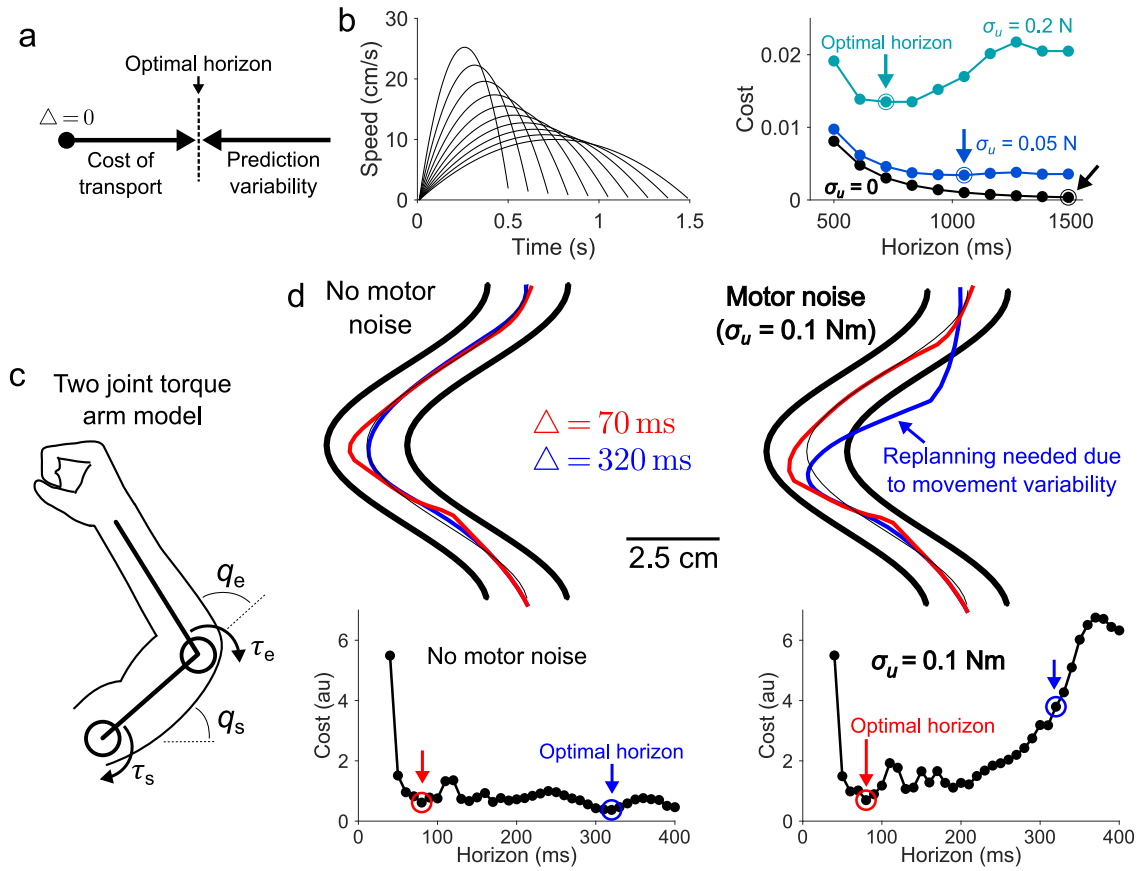

Figure 4: IPC's optimal horizon depends on the cost of transport and prediction variability. (a) Minimizing the cost of transport leads to a longer horizon, but variability in the prediction error shortens it, yielding an optimal horizon. (b) Simulations of reaching with IPC for different horizons to the same target location 10 cm away ($p_S = 0$ and $p_T = 100\,\mathrm{cm}^2$). As motor noise gradually increased ($\sigma_u = 0$ in black, $\sigma_u = 0.05\,\mathrm{N}$ in blue, and $\sigma_u = 0.2\,\mathrm{N}$ in teal) the horizon yielding the smallest cost became shorter. (c) A two joint model of the arm with elbow and shoulder joints was used to simulate the effect of world model inaccuracy on the optimal horizon. (d) IPC with no motor noise (left) and motor noise $\sigma_u = 0.1\,\mathrm{Nm}$ (right) moving through a narrow path with walls (thick traces). With no motor variability (left), the cost was minimized by planning with a longer horizon of $\triangle = 320\,\mathrm{ms}$ (blue). A shorter horizon yielded a more intermittent movement that strayed from the center of the path (red). But when motor noise was introduced, a shorter horizon yielded a less costly movement overall relative to a longer horizon as the latter strayed greatly from the path due to an accumulation of error.

Besides complementary costs, an important factor affecting the optimal horizon is the uncertainty in the prediction. To illustrate this, we simulated the effect of uncertainty when controlling a two-joint arm with elbow and shoulder torques (see Fig. 4c). In the simulation, the objective was to follow a target trajectory for $400\,\mathrm{ms}$ as it passed between two walls (Fig. 4d, top left). The horizon was defined as the amount of available information regarding the target trajectory, which depends on how much of it (in ms) is visible ahead of the current time. For example, a $40\,\mathrm{ms}$ horizon meant that only a tenth of the total target trajectory was visible ahead from the current time.

To illustrate the effect of uncertainty on the optimal planning horizon, we first consider that IPC only replanned after fully executing its open-loop plan, without using the information-based replanning previously introduced (see next Section for simulations including both the replanning and the optimization of the horizon). Uncertainty was introduced by simulating an additive motor noise with variance $p_u = \sigma_u^2$ in the movement dynamics (accounted for by p_M).

First, when $p_M \equiv 0$, a long horizon ($\triangle = 320\,\mathrm{ms}$) yielded the optimal cost of movement as IPC could plan most of the movement at once without needing to replan. This long horizon resulted in a smooth movement that optimally accounted for the target's curvature (Fig. 4d, blue trajectory in top left). Conversely, with a short horizon ($\triangle = 70\,\mathrm{ms}$) IPC had to constantly correct its planning with less knowledge of the target's curvature, resulting in overshoots and jerky motions at the junction of planned segments (Fig. 4d, red trajectory in top left).

Second, in presence of additive motor noise, a long horizon was detrimental to task performance as IPC veered from the target trajectory due to the time-accumulation of noise corrupting the plan's execution (Fig. 4d, blue in top right). A shorter horizon ($\triangle = 70\,\mathrm{ms}$) was beneficial in this case as IPC could correct movement errors due to motor noise on-the-fly (Fig. 4d, red in top right). These illustrate how the optimal horizon should depend on the task parameters, with the aim of minimizing the number of necessary replanning steps (known to be costly [38]) and the overall cost of transport. Therefore, a mechanism should be implemented to adjust the horizon as the task unfolds, which we describe in the following subsection on the scenario of a hunter catching an agile prey. Importantly, our simulations are consistent with the results of [39], who found that the horizon was shorter for novices as for experts during a similar path tracking task. This suggests that experts, who are more likely to properly compensate their motor variability [40], can leverage a longer horizon.

2.5 Replanning and optimizing a hunter's movements

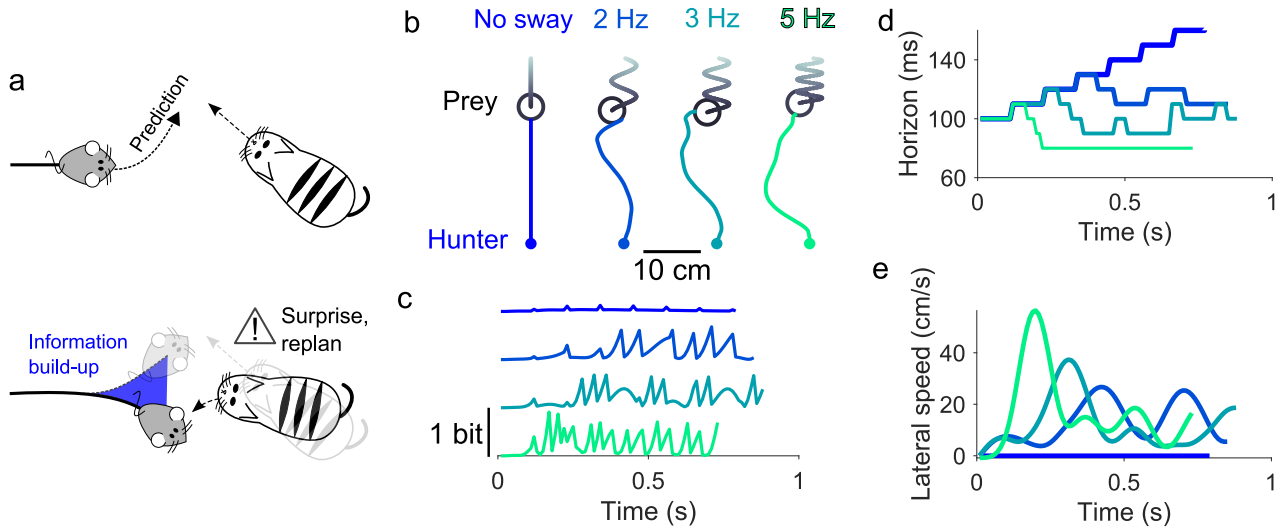

Figure 5: Simulation of a hunter intercepting a prey in a plane. The simulations were performed with $p_T = 3\,\mathrm{cm}^2$ and $p_S = 1\,\mathrm{cm}^2$. (a) Cat trying to intercept a mouse using IPC. The movement is replanned when the prediction error exceeds the permissible variance. As the prey's movement grows more unpredictable, surprise builds-up more quickly, thereby triggering replanning more often. (b) The frequency of the prey's lateral sway was increased to vary the goal's variability (shaded colors show the progression from lighter to darker). Hunter and prey's trajectories are shown up until the time when the distance between the hunter and prey falls below p_T. Intercepting the prey becomes more difficult as its movement becomes more unpredictable. Lower left panel shows the information as a function of time for each prey (offset added to vertical axis for visibility). As the predictability of the prey's movement decreased, information builds up more rapidly, triggering replanning. Lower right panel shows the length of the horizon, which shortened as the prey's movement grew more unpredictable due to more frequent replanning.

Since replanning is costly [38], we propose that the brain would iteratively adjust the horizon depending on the experience with past replanning intervals, so as to avoid superfluous replanning. If the information associated with the prediction error frequently exceeds I_T, replanning will occur often and it would be inefficient to plan long term actions, thus the horizon should be shortened. Conversely, if I_T is rarely exceeded, then replanning occurs less frequently, hence a longer horizon can be used. Therefore, we propose the iterative adjustment of the horizon

$$\triangle_{i+1} = \beta\triangle_i + (1-\beta)r + \gamma, \text{ with } 0 \leq \beta \leq 1 \text{ and } \gamma \geq 0 \tag{5}$$

After each replanning, the next horizon $\triangle_{i+1}$ is adapted as a convex combination of the current horizon $\triangle_i$ and the time elapsed since the last replanning r depending on β. γ is a confidence parameter that tends to extend the horizon.

To illustrate the combined effects of the information-based replanning with planning horizon adaptation, we simulate the scenario of a hunter tracking a prey's movement in a plane (Fig. 5a). Notably, this scenario incorporates all the elements of IPC, from the task admissible variance (represented by the prey size) to the uncertainty in the evolution of the environment. Specifically, we adjusted the prey's sway along the horizontal axis using a sine function with frequency $f \in \{0, 2, 3, 5\}$ Hz, making the prey difficult to catch due to the increased goal variability p_G (Fig. 5b). The initial planning horizon was $\triangle_0 = 100\,\text{ms}$ and we used $\beta = 0.7$ and $\gamma = 10\,\text{ms}$ for all simulations. Without any lateral sway (i.e. $f = 0\,\text{Hz}$), IPC gradually increased its planning horizon as the prey's movement was predictable. Conversely, when the prey's lateral sway frequency increased, the horizon gradually decreased (Fig. 5c, top right panel) as the prey's movements were less predictable, leading to higher rates of information-based replanning (Fig. 5b, bottom panel). Importantly, this increase in the number of replanning events affected the number of submovements, as illustrated by the peaks in the lateral component of the hunter's speed (Fig. 5e, bottom right panel), consistent with the initial principles that guided the development of IPC.

3 Discussion

The Information Predictive Control introduced in this paper is a computational framework to explain how the brain plans and executes movements under time-varying goals. IPC integrates an information module with model predictive control [27, 41] enabling replanning when deviations from expected states become sufficiently surprising, i.e., when they contain sufficient information. By combining control and information theory, IPC accounts for reactive behaviors beyond what Optimal Feedback Control can explain. Furthermore, it addresses the limitations of previous models of intermittency that did not consider how task tolerance and sensory, motor and goal noise influence the rate of replanning [17, 21–24]. Therefore, IPC explains and reproduces century-old observations of intermittency in movement control, whether in discrete [18, 42] and continuous human movements [43, 44] or in other species such as cats [15], mice [16], and non-human primates [20]. This intermittency has been proposed to stem from a brain sensitive to errors only above a certain threshold [45, 46] or be triggered by alpha waves [21]. However, these hypotheses did not account for the influence of sensory, motor, and goal noise on the replanning frequency.

In the IPC framework, when the prediction error exceeds its permissible variance, the generated information triggers movement replanning. Since replanning a movement entails metabolic [38] and cognitive [47] costs and can impair motor performance [48], IPC minimizes the number of replanning events by considering several factors. First, large sensory noise in vision or proprioception increases the permissible variance in the prediction error, as the error estimates become less reliable. Consequently, IPC reduces the replanning frequency when sensory information is noisy, consistent with the findings in [25] that intermittency decreases when tracking a target with noisy peripheral visual feedback. Second, the sum of motor and goal variability in the permissible variance is capped by the task tolerance, i.e., the accuracy constraints of the task. Greater motor or goal variability will reduce the replanning frequency as long as the task tolerance is high, meaning that large deviations along task-irrelevant directions are neglected [13, 31]. However, if the task tolerance is low, or with high accuracy constraints, larger motor or goal variability raises the replanning frequency, as even small deviations in the prediction error trigger replanning. This minimum intervention principle has been described through the concept of the uncontrolled manifold, according to which only degrees of freedom (DoF) relevant to the task are controlled [49, 50]. While OFC also avoids intervening along task-irrelevant DoFs, it intervenes along the task-relevant dimension, regardless of the error magnitude or target reachability. In contrast, IPC intervenes only when the error is substantial enough to warrant replanning and the target is likely reachable. IPC thus extends and refines the minimum intervention principle by distinguishing intervention needs along task-relevant as well as

task-irrelevant dimensions.

Our simulations show how the planning horizon—the duration into the future considered when planning a movement—emerges as a property tied to the replanning frequency. When only the cost of movement was considered in IPC, the optimal horizon extended toward infinity as slower movements were least costly. In practice, movement's duration is limited, which can be modeled via a reward discounted with time yielding an optimal movement duration [51, 52]. Experimental evidence also suggests that very slow movements may be as costly for the brain as very fast, effortful, ones [53, 54]. In our approach, instead uncertainty in the prediction error naturally limits the planning horizon, consistent with variance-minimization frameworks [11, 18, 37].

Throughout the paper, we showed how inaccuracies in the world model promote a shorter planning horizon, as frequent replanning reduces the overall task cost. This prediction aligns with findings from a study in which participants had to move a cursor along a narrow path [39]. Novice participants employed a short planning horizon, likely due to the need for frequent error corrections. In contrast, experienced participants used a longer horizon, possibly by leveraging task knowledge acquired through practice that reduced execution errors and replanning needs. The adaptive mechanism similarly increased the horizon in predictable conditions and reduced it when task uncertainty increased, as illustrated in the hunting example. This mechanism could explain why movement intermittency increases and the duration of submovements decreases when approaching a small target [55].

While we used a surprise threshold to trigger replanning, our approach can be extended by incorporating principles of decision-making. For instance, a drift-diffusion model could trigger replanning based on accumulated information over time [56], which could make IPC more robust to false alarms and enable it to correct permissible but persistent prediction errors.

A significant advantage of IPC is the flexibility of the underlying internal model, which can be linear or non-linear, take any form from differential equations to neural networks, as long as it can predict the future internal and environment's state. This work focused on IPC's properties, but learning of the internal model could be integrated through feedback minimization [35] or reinforcement learning [57]. As the internal model better compensates for the environment dynamics, it will yield more accurate predictions, thereby reducing replanning events. Furthermore, IPC's flexibility in modeling the cost minimized by the brain can incorporate factors such as the movement timing and reward discussed above. Importantly, it can also consider system stochasticity to predict key motor control features like feedforward control of motion [18] and cocontraction [9].

Overall, IPC's ability to produce and correct movement trajectories based on an internal model, information theory, and a flexible formulation of the brain's internal costs, make it a useful tool for computational neuroscientists to emulate and investigate how the brain's control movements in a dynamic environment.

4 Methods and Materials

Information Predictive Control (IPC) uses an internal model to plan the future control inputs $\mathbf{u}$ needed to accomplish a given goal over a *time horizon* $\triangle$. Here we describe how IPC works on the simulations described in the paper.

Information Predictive Control of a linear system

We first simulate reaching movements using an arm modeled as a point mass in two dimensions x and y (as illustrated in Figure 2). The arm moves according to the linear dynamics

$$\dot{\boldsymbol{\xi}} = \mathbf{A}\boldsymbol{\xi} + \mathbf{B}(\mathbf{u} + \mathbf{F}_e)\,, \;\; \boldsymbol{\xi} = \begin{bmatrix} x \\ y \\ \dot{x} \\ \dot{y} \end{bmatrix}, \;\; \mathbf{A} = \begin{bmatrix} 0 & 0 & 1 & 0 \\ 0 & 0 & 0 & 1 \\ 0 & 0 & 0 & 0 \\ 0 & 0 & 0 & 0 \end{bmatrix}, \;\; \mathbf{B} = \begin{bmatrix} 0 & 0 \\ 0 & 0 \\ 1/m & 0 \\ 0 & 1/m \end{bmatrix} \tag{6}$$

where $\boldsymbol{\xi}, \mathbf{u}, \mathbf{F}_e$ are functions of time t and $m = 1\,\mathrm{kg}$. $\mathbf{F}_e$ is the force from the environment, which is $\mathbf{0}$ in the free condition, or

$$\mathbf{F}_e = \begin{bmatrix} -1 & -1 \\ -1 & 1 \end{bmatrix} \begin{bmatrix} \dot{x} \\ \dot{y} \end{bmatrix} \tag{7}$$

as a velocity-dependent force field, where $\mathbf{F}_e$ is in N and $\dot{x}, \dot{y}$ in m/s. The goal is to move state $\boldsymbol{\xi}(t)$ at current time t to the goal $\boldsymbol{\xi}^*(t^+)$ at $t^+ \equiv t + \triangle$ using a force $\mathbf{u}(\zeta) = [u_x(\zeta), u_y(\zeta)]'$, $\zeta \in [t, t^+]$, by minimizing the cost function

$$V(t) = \left[\tilde{\boldsymbol{\xi}}(t^+) - \tilde{\boldsymbol{\xi}}^*(t^+)\right]' \mathbf{Q} \left[\tilde{\boldsymbol{\xi}}(t^+) - \tilde{\boldsymbol{\xi}}^*(t^+)\right] + \int_t^{t^+} \mathbf{u}'(\zeta)\, \mathbf{R}\, \mathbf{u}(\zeta)\, dt\,, \quad t^+ \equiv t + \triangle\,. \tag{8}$$

The first term weighted by $\mathbf{Q}$ is to ensure that the predicted state $\tilde{\boldsymbol{\xi}}$ comes close to the predicted goal $\tilde{\boldsymbol{\xi}}^*$ at the horizon, the second term to minimize effort.

The future state $\tilde{\boldsymbol{\xi}}$ is computed by integrating Eq. 6. The future $\tilde{\boldsymbol{\xi}}^*$ is estimated using linear quadratic estimation [58], starting from their last measured value at time t. For this purpose, the goal state is assumed to evolve according to $\dot{\tilde{\boldsymbol{\xi}}}^* = \mathbf{A}\tilde{\boldsymbol{\xi}}^*$and observed with

$$\mathbf{z}^* = \begin{bmatrix} x^* \\ y^* \end{bmatrix} + \boldsymbol{\eta}\,, \quad \boldsymbol{\eta} \in G(\mathbf{0}, \mathbf{P}_S) \tag{9}$$

where $\mathbf{P}_S$ is the sensory noise covariance matrix.

The future control inputs $\mathbf{u}$ to minimize the cost of Eq. 8 were optimized by Quadratic Programming (QP) where the control inputs were iteratively updated until the solution converged to an acceptable minimum. There are several algorithms for solving QP class problems, and the one we adopted was the interior-point method implemented in Matlab's '*fmincon*' function due to its speed and robustness. The last control input was bounded to be equal to $\mathbf{0}$ to avoid discontinuities between movements and to keep IPC passive when time exceeded the horizon.

Above equations were discretized with a 1 ms time step for all simulations. In the simulations of Fig. 2b,c , (solid blue and dashed blue), reaching movements were simulated from the origin $\mathbf{x}_0 = [0, 0]'$ toward a target located at [0,0.1] m using $p_e = 9\,\mathrm{cm}^2$, $\triangle = 700\,\mathrm{ms}$, $\mathbf{Q}$ = diag(5,5,1,1) and $\mathbf{R} = 10^{-5} I_2$, where I_2 is the 2×2 identity matrix. The same parameters were used to simulate the movements in Fig. 3d,e with $p_e = 1\,\mathrm{cm}^2$ and $p_e = 4\,\mathrm{cm}^2$, respectively. For Fig. 4b we simulated 30 reaching movements with the same parameters as above while the horizon $\triangle$ was varied between $[500, 1490]\,\mathrm{ms}$ in steps of $110\,\mathrm{ms}$. For these simulations, constant motor noise was added to the motor command: $\mathbf{u} + \boldsymbol{\nu}$, $\boldsymbol{\nu} \in G\big(\mathbf{0}, \sigma_u^2 I_2\big)$, where 10 movements were simulated with $\sigma_u = 0\,\mathrm{N}$, another 10 with $\sigma_u = 0.05\,\mathrm{N}$ and the final 10 with $\sigma_u = 0.2\,\mathrm{N}$.

For the simulations in Fig. 5b-e, the horizon was initially set to $\triangle = 100\,\mathrm{ms}$ then adapted according to eq. (5) with $\beta = 0.7$ and $\gamma = 10\,\mathrm{ms}$. The other parameters were $p_e = 4\,\mathrm{cm}^2$, $\mathbf{Q}$ = diag(10^3,10^3,10,10) and $\mathbf{R} = 10^{-1} I_2$. The prey moved according to

$$\begin{bmatrix} x^*(t) \\ y^*(t) \end{bmatrix} = \begin{bmatrix} 0.02 \sin(2\pi f t) \\ 0.3 - 0.1\, t \end{bmatrix} \tag{10}$$

where the frequency f was selected from the set $\{0, 2, 3, 5\}$ Hz.

The feedback gains of the Optimal Feedback Controller in Fig. 2b,c (solid red line) were computed backwards through the Riccati equation. This was used in Eq. 6 to simulate the system under OFC as explained e.g. in [59].

Simulation of wrist tracking movement

The wrist tracking data of Fig. 3 came from an exemplar participant who used their right wrist to track a target trajectory [36], that was computed as a linear combination of four sine functions

$$x^*(t) = -7.8 \sin(0.12\, t) + 1.6 \sin(0.28\, t) + 9.4 \sin(0.37\, t) - 10.6 \sin(0.64\, t) \tag{11}$$

where t is the time. We extracted five seconds of data from within an exemplary trial which showed the submovements during tracking.

IPC tracked the target movement along the single x dimension using the cost function

$$V(t) = \int_t^{t^+} \mathbf{u}'(t)\, \mathbf{R}\, \mathbf{u}(t) + \left[\tilde{\boldsymbol{\xi}}(t) - \tilde{\boldsymbol{\xi}}^*(t)\right]' \mathbf{Q} \left[\tilde{\boldsymbol{\xi}}(t) - \tilde{\boldsymbol{\xi}}^*(t)\right] dt \tag{12}$$

where $\triangle = 250\,\mathrm{ms}$, $\mathbf{Q}$ = diag(100,1) and $R = 10^{-5}$. The wrist was simulated as a 0.5 kg point mass moving in one dimension. In the tracking simulation, $p_T = 8\,\mathrm{cm}^2$ with small sensory noise $p_S = 8\,\mathrm{cm}^2$ or large sensory noise $p_S = 56\,\mathrm{cm}^2$.

The feedback gain for OFC was constant and set to [100,30]' to track the target.

Simulation of two-joint arm control

The effect of model inaccuracy on IPC's behavior was simulated in Fig. 4d using a model horizontal arm movement around the shoulder and elbow with joint angles $\mathbf{q} = [q_s, q_e]'$ controlled by the torques $\boldsymbol{\tau} = [\tau_s, \tau_e]'$ (Fig. 4c), having dynamics

$$\boldsymbol{\tau} = \mathbf{M}\,\ddot{\mathbf{q}} + \mathbf{C}\,\dot{\mathbf{q}}\,, \quad \mathbf{M} = \begin{bmatrix} I_s + I_e + \kappa\, c_e & \kappa\, c_e \\ \kappa\, c_e & I_e \end{bmatrix}, \tag{13}$$
$$\mathbf{C} = \kappa\, s_e \begin{bmatrix} -2\dot{q}_e & \dot{q}_e \\ \dot{q}_s & 0 \end{bmatrix}, \quad \kappa = 0.5\, m_e\, l_s\, l_e \quad c_e \equiv \cos q_e \quad s_e \equiv \sin q_e\,.$$

We used the parameters from [58]: $l_s = 0.3\,\mathrm{m}$ and $l_e = 0.35\,\mathrm{m}$ for the lengths of the shoulder and elbow segments, $I_s = 0.05\,\mathrm{kg\,m^2}$ and $I_e = 0.06\,\mathrm{kg\,m^2}$ their moments of inertia, and $m_s = 1.9\,\mathrm{kg}$ and $m_e = 1.7\,\mathrm{kg}$ their masses. The joint inertia was computed assuming that the elbow's center of mass is in the middle of its segment.

The state $\boldsymbol{\xi} = [\mathbf{q}, \dot{\mathbf{q}}]'$ was controlled to track the Cartesian goal trajectory in the middle of the path

$$\begin{bmatrix} x^*(t) \\ y^*(t) \end{bmatrix} = \begin{bmatrix} 0.025\sin(5\pi t) - 0.1 \\ 0.25\, t \end{bmatrix} \tag{14}$$

which was converted to joint coordinates via the arm's inverse kinematics

$$\mathbf{q}^*(t) = \begin{bmatrix} \mathrm{Atan2}\left[y^*(t), x^*(t)\right] - \arccos\left(\frac{(x^*(t))^2 + (y^*(t))^2 + l_s^2 - l_e^2}{2\, l_s \sqrt{(x^*(t))^2 + (y^*(t))^2}}\right) \\ \\ \arccos\left(\frac{(x^*(t))^2 + (y^*(t))^2 - l_s^2 - l_e^2}{2\, l_s\, l_e}\right). \end{bmatrix} \tag{15}$$

to yield $\boldsymbol{\xi}^*(t) = [\mathbf{q}^*(t), \dot{\mathbf{q}}^*(t)]'$. This goal state was tracked by minimizing cost function Eq. 12 with $\mathbf{Q} = \mathrm{diag}(10^3, 10^{-2})$ and $\mathbf{R} = 10^{-3} I_2$. The horizon was incrementally changed from 40 ms to 400 ms in steps of 10 ms. The prediction error was set to a large value $p_e = 100\,\mathrm{cm}^2$ so that movement replanning was suppressed in these simulations.

Acknowledgments

The authors would like to thank Yasuharu Koike and Hiroaki Gomi for discussions.

Competing interests

The authors have no competing financial or non-financial interests.

Materials & Correspondence

Correspondence and requests for material should be sent to A.T.

References

[1] W. L. Nelson, "Physical principles for economies of skilled movements," Biological Cybernetics, vol. 46, pp. 135–147, feb 1983.

[2] T. Flash and N. Hogan, "The coordination of arm movements: an experimentally confirmed mathematical model," The Journal of Neuroscience, vol. 5, pp. 1688–1703, jul 1985.

[3] Y. Uno, M. Kawato, and R. Suzuki, "Formation and control of optimal trajectory in human multijoint arm movement," Biological Cybernetics, vol. 61, pp. 89–101, jun 1989.

[4] E. Nakano, H. Imamizu, R. Osu, Y. Uno, H. Gomi, T. Yoshioka, and M. Kawato, "Quantitative examinations of internal representations for arm trajectory planning: minimum commanded torque change model," Journal of Neurophysiology, vol. 81, pp. 2140–2155, may 1999.

[5] A. Biess, D. G. Liebermann, and T. Flash, "A computational model for redundant human three-dimensional pointing movements: integration of independent spatial and temporal motor plans simplifies movement dynamics," Journal of Neuroscience, vol. 27, pp. 13045–13064, nov 2007.

[6] S. Ben-Itzhak and A. Karniel, "Minimum acceleration criterion with constraints implies bang-bang control as an underlying principle for optimal trajectories of arm reaching movements," Neural Computation, vol. 20, pp. 779–812, Mar. 2008.

[7] B. Berret, E. Chiovetto, F. Nori, and T. Pozzo, "Evidence for composite cost functions in arm movement planning: an inverse optimal control approach," PLoS Computational Biology, vol. 7, no. 10, pp. 1–18, 2011.

[8] B. Berret and F. Jean, "Stochastic optimal open-loop control as a theory of force and impedance planning via muscle co-contraction," PLOS Computational Biology, vol. 16, p. e1007414, Feb. 2020.

[9] B. Berret, D. Verdel, E. Burdet, and F. Jean, "Co-contraction embodies uncertainty: an optimal feedforward strategy for robust motor control," PLOS Computational Biology, vol. 20, no. 11, p. e1012598, 2024.

[10] M. Kawato, "Internal models for motor control and trajectory planning," Current Opinion in Neurobiology, vol. 9, pp. 718–727, dec 1999.

[11] C. M. Harris and D. M. Wolpert, "Signal-dependent noise determines motor planning," Nature, vol. 394, pp. 780–784, aug 1998.

[12] A. Takagi, S. Ito, and H. Gomi, "Minimizing command timing volatility is a key factor in skilled actions," bioRχiv, June 2024.

[13] E. Todorov and M. I. Jordan, "Optimal feedback control as a theory of motor coordination," Nature Neuroscience, vol. 5, pp. 1226–1235, nov 2002.

[14] S. H. Scott, "The computational and neural basis of voluntary motor control and planning," Trends in Cognitive Sciences, vol. 16, pp. 541–549, Nov. 2012.

[15] J. H. Martin, S. E. Cooper, and C. Ghez, "Kinematic analysis of reaching in the cat," Experimental Brain Research, vol. 102, no. 3, 1995.

[16] M. I. Becker, D. J. Calame, J. Wrobel, and A. L. Person, "Online control of reach accuracy in mice," Journal of Neurophysiology, vol. 124, pp. 1637–1655, Dec. 2020.

[17] A. Vallbo and J. Wessberg, "Organization of motor output in slow finger movements in man.," The Journal of physiology, vol. 469, no. 1, pp. 673–691, 1993.

[18] E. Burdet and T. E. Milner, "Quantization of human motions and learning of accurate movements," Biological Cybernetics, vol. 78, pp. 307–318, May 1998.

[19] A. Takagi, H. Kambara, and Y. Koike, "Reduced effort does not imply slacking: responsiveness to error increases with robotic assistance," IEEE Transactions on Neural Systems and Rehabilitation Engineering, vol. 26, pp. 1363–1370, July 2018.

[20] A. Fishbach, S. A. Roy, C. Bastianen, L. E. Miller, and J. C. Houk, "Kinematic properties of on-line error corrections in the monkey," Experimental Brain Research, vol. 164, pp. 442–457, June 2005.

[21] E. Guigon, "A computational theory for the production of limb movements.," Psychological Review, aug 2021.

[22] P. D. Neilson, M. D. Neilson, and N. J. O'Dwyer, "Internal models and intermittency: A theoretical account of human tracking behavior," Biological Cybernetics, vol. 58, pp. 101–112, Jan. 1988.

[23] P. J. Gawthrop and L. Wang, "Intermittent model predictive control," Proceedings of the Institution of Mechanical Engineers, Part I: Journal of Systems and Control Engineering, vol. 221, pp. 1007–1018, Nov. 2007.

[24] Y. Sakaguchi, M. Tanaka, and Y. Inoue, "Adaptive intermittent control: A computational model explaining motor intermittency observed in human behavior," Neural Networks, vol. 67, pp. 92–109, July 2015.

[25] D. W. Reed, X. Liu, and R. C. Miall, "On-line feedback control of human visually guided slow ramp tracking: effects of spatial separation of visual cues," Neuroscience Letters, vol. 338, pp. 209–212, Mar. 2003.

[26] J. Richalet, "Industrial applications of model based predictive control," Automatica, vol. 29, pp. 1251–1274, Sept. 1993.

[27] A. Takagi, H. Gomi, E. Burdet, and Y. Koike, "A model predictive control strategy to regulate movements and interactions," bioRχiv, Aug. 2022.

[28] C. E. Shannon, "A mathematical theory of communication," ACM SIGMOBILE Mobile Computing and Communications Review, vol. 5, pp. 3–55, Jan. 2001.

[29] K. Takiyama, M. Hirashima, and D. Nozaki, "Prospective errors determine motor learning," Nature Communications, vol. 6, Jan. 2015.

[30] D. J. Herzfeld, P. A. Vaswani, M. K. Marko, and R. Shadmehr, "A memory of errors in sensorimotor learning," Science, vol. 345, pp. 1349–1353, Sept. 2014.

[31] E. Todorov and M. Jordan, "A minimal intervention principle for coordinated movement," Advances in neural information processing systems, vol. 15, 2002.

[32] M. Bar, Predictions in the brain: Using our past to generate a future. Oxford University Press, 2011.

[33] T. Parr, G. Pezzulo, and K. J. Friston, Active inference: the free energy principle in mind, brain, and behavior. MIT Press, 2022.

[34] R. Shadmehr and F. A. Mussa-lvaldi, "Adaptive representation of dynamics during learning of a motor task," Journal of Neuroscience, vol. 14, pp. 3208–3224, May 1994.

[35] D. W. Franklin, E. Burdet, K. P. Tee, R. Osu, C.-M. Chew, T. E. Milner, and M. Kawato, "CNS learns stable, accurate, and efficient movements using a simple algorithm," The Journal of Neuroscience, vol. 28, pp. 11165–11173, Oct. 2008.

[36] A. Takagi, F. Usai, G. Ganesh, V. Sanguineti, and E. Burdet, "Haptic communication between humans is tuned by the hard or soft mechanics of interaction," Computational Biology, vol. 14, pp. 1–17, Mar. 2018.

[37] B. Berret, A. Conessa, N. Schweighofer, and E. Burdet, "Stochastic optimal feedforward-feedback control determines timing and variability of arm movements with or without vision," PLOS Computational Biology, vol. 17, p. e1009047, jun 2021.

[38] E. Sedaghat-Nejad and R. Shadmehr, "The cost of correcting for error during sensorimotor adaptation," Proceedings of the National Academy of Sciences, vol. 118, Sept. 2021.

[39] L. Bashford, D. Kobak, J. Diedrichsen, and C. Mehring, "Motor skill learning decreases movement variability and increases planning horizon," Journal of Neurophysiology, vol. 127, pp. 995–1006, Apr. 2022.

[40] L. Shmuelof, J. W. Krakauer, and P. Mazzoni, "How is a motor skill learned? change and invariance at the levels of task success and trajectory control," Journal of Neurophysiology, vol. 108, pp. 578–594, July 2012.

[41] S. Katayama, M. Murooka, and Y. Tazaki, "Model predictive control of legged and humanoid robots: models and algorithms," Advanced Robotics, vol. 37, pp. 298–315, Feb. 2023.

[42] R. S. Woodworth, "Accuracy of voluntary movement.," The Psychological Review: Monograph Supplements, vol. 3, no. 3, pp. i–114, 1899.

[43] R. C. Miall, D. J. Weir, and J. F. Stein, "Intermittency in human manual tracking tasks," Journal of Motor Behavior, vol. 25, pp. 53–63, Mar. 1993.

[44] M. A. Vince, "The intermittency of control movements and the psychological refractory period," British Journal of Psychology, vol. 38, no. 3, p. 149, 1948.

[45] P. Gawthrop, I. Loram, M. Lakie, and H. Gollee, "Intermittent control: a computational theory of human control," Biological Cybernetics, vol. 104, pp. 31–51, Feb. 2011.

[46] D. M. Wolpert, R. C. Miall, J. L. Winter, and J. F. Stein, "Evidence for an error deadzone in compensatory tracking," Journal of Motor Behavior, vol. 24, pp. 299–308, Dec. 1992.

[47] M. A. Spiegel, D. Koester, M. Weigelt, and T. Schack, "The costs of changing an intended action: Movement planning, but not execution, interferes with verbal working memory," Neuroscience Letters, vol. 509, pp. 82–86, Feb. 2012.

[48] J.-J. Orban de Xivry and P. Lefèvre, "A switching cost for motor planning," Journal of Neurophysiology, vol. 116, pp. 2857–2868, Dec. 2016.

[49] J. P. Scholz and G. Schöner, "The uncontrolled manifold concept: identifying control variables for a functional task," Experimental Brain Research, vol. 126, pp. 289–306, May 1999.

[50] D. Campolo, F. Widjaja, H. Xu, W. T. Ang, and E. Burdet, "Analysis of accuracy in pointing with redundant hand-held tools: a geometric approach to the uncontrolled manifold method," PLoS Computational Biology, vol. 9, p. e1002978, Apr. 2013.

[51] L. Rigoux and E. Guigon, "A model of reward- and effort-based optimaldecision making and motor control," PLoS Computational Biology, vol. 8, pp. 1–13, Jan. 2012.

[52] R. Shadmehr, H. J. Huang, and A. A. Ahmed, "A representation of effort in decision-making and motor control," Current Biology, vol. 26, pp. 1929–1934, jul 2016.

[53] B. Berret and G. Baud-Bovy, "Evidence for a cost of time in the invigoration of isometric reaching movements," Journal of Neurophysiology, vol. 127, pp. 689–701, feb 2022.

[54] D. Verdel, O. Bruneau, G. Sahm, N. Vignais, and B. Berret, "The value of time in the invigoration of human movements when interacting with a robotic exoskeleton," Science Advances, vol. 9, sep 2023.

[55] T. E. Milner, "A model for the generation of movements requiring endpoint precision," Neuroscience, vol. 49, pp. 487–496, July 1992.

[56] R. Ratcliff, "A theory of memory retrieval.," Psychological Review, vol. 85, no. 2, pp. 59–108, 1978.

[57] K. Doya, K. Samejima, K.-i. Katagiri, and M. Kawato, "Multiple Model-Based Reinforcement Learning," Neural Computation, vol. 14, pp. 1347–1369, June 2002.

[58] W. Li and E. Todorov, "Iterative linear quadratic regulator design for nonlinear biological movement systems.," in International Conference on Informatics in Control, Automation and Robotics (ICINCO), pp. 222–229, Citeseer, 2004.

[59] A. Takagi, N. Beckers, and E. Burdet, "Motion plan changes predictably in dyadic reaching," PLOS ONE, vol. 11, p. e0167314, Dec. 2016.